Asian Journal of Chemistry; Vol. 36, No. 7 (2024), 1705-1712

ASIAN JOURNAL OF CHEMISTRY

https://doi.org/10.14233/ajchem.2024.31775

Antibacterial and Antiviral Potential of Zirconium Oxide Nanoparticle using Extract of *Chloranthus erectus* Leaf

Nor' Aishah Hasan[1,], Nurul Natasha Wazir[1], Nurhamimah Zainal-Abidin[1,], Mohd Zaini Nawahwi[1,], Nurul Atikah Badrol Hisham[2], Yamin Yasin[2], Nik Rozlin Nik Masdek[3,], Jasmine Elanie Khairat[4,], Lim Zhi Yu[4], Azzreena Mohamad Azzeme[5,], Syukri Arief[6,], Gusliani Eka Putri[7,] and Nor Monica Ahmad[2,*,]

[1]School of Biology, Faculty of Applied Sciences, Universiti Teknologi MARA, Cawangan Negeri Sembilan, Kampus Kuala Pilah, 72000 Kuala Pilah, Malaysia
[2]School of Chemistry and Environment, Faculty of Applied Sciences, Universiti Teknologi MARA, Cawangan Negeri Sembilan, Kampus Kuala Pilah, 72000 Kuala Pilah, Malaysia
[3]School of Mechanical Engineering,College of Engineering 40450 UiTM,Shah Alam, Selangor, Malaysia
[4]Institute of Biological Sciences, Faculty of Science, Universiti Malaya, Kuala Lumpur 50603, Malaysia
[5]Department of Biochemistry, Faculty of Biotechnology and Biomolecular Sciences, Universiti Putra Malaysia, 43400 UPM Serdang, Selangor, Malaysia
[6]Faculty of Mathematics and Natural Sciences, Andalas University, Padang, Indonesia
[7]Department of Medical Laboratory Technology, Syedza Saintika College of Health Sciences, Padang, Indonesia

*Corresponding author: E-mail: normonica@gmail.com; normonica@uitm.edu.my

Received: 30 April 2024; *Accepted*: 20 June 2024; *Published online*: 29 June 2024; AJC-21690

Zirconium oxide nanoparticles (ZrO_2 NPs) were synthesized with an effective capping agent using aqueous extract of *Chlorentus erectus* at the optimized conditions. The aqueous leaf extract contained phytochemical compounds that could regulate the size and shape of the nanoparticles. The average size of *C. erectus*-ZrO_2 NPs crystallite was 10.42 nm, which was determined based on Scherrer Debye's equation. The finding indicated the effectiveness of the phytochemical compounds to diminish the agglomeration of the particles. The *C. erectus* mediated ZrO_2 NPs were in spherical clusters when observed through a transmission electron microscope (TEM). An elemental energy diffraction X-ray (EDX) assessment also revealed a significant zirconium and oxygen percentage, suggesting that the phytochemicals present in the leaf extract did not alter the purity of *C. erectus*-ZrO_2 NPs. Moreover, 200 µg/mL of synthesized ZrO_2 NPs effectively inhibited *K. pneumoniae*. Up to 300 µg/mL of *C. erectus*- ZrO_2 NPs demonstrated non-toxicity to vero cells and low antiviral properties against the DENV-2 virus when introduced to cells post-infection.

Keywords: Capping agent, *Chlorentus erectus*, Nanoparticles, Synthesis, Zirconium oxide.

INTRODUCTION

Zirconium oxide nanoparticles (ZrO_2 NPs) possess excellent attributes due to their significant stability, biocompatibility and band gap. Consequently, ZrO_2 NPs are extensively employed in various applications, including in producing photocatalysts [1], biosensors [2], antifungal [3] and antibacterial [4]. The ZrO_2 NPs are synthesized through several processes, including chemical approaches, such as precipitation, sol-gel and hydrothermal and microwave-assisted. Yadav *et al.* [5] also suggested a hydrothermal method of obtaining high-quality ZrO_2 NPs. The study only employed precursor chemicals and precipitation agents. The generated samples were 30 nm, which fulfilled the nano-size criterion and agglomerated with a spherical cluster. Tantuvoy *et al.* [6] documented similar findings when utilizing similar chemicals and the microwave irradiation method.

Recently, capping agents and surfactants have demonstrated abilities to produce nanoparticles with controllable shapes and sizes when applied during nanoparticles synthesis. For instance, Tapak *et al.* [2] prepared ZrO_2 NPs with 1-butyl-3-methylimidazolium trifluoroacetate as a capping agent to obtain superior NPs (10.60 nm) with less spherical clusters. In another study,

Ordóñez *et al.* [7] synthesized ZrO_2 NPs with different surfactants, sodium dodecyl benzene sulfonate and hexadecyltrimethylammonium bromide and polyvinylpyrrolidone as a stabilizer to improve the nanoparticles dispersion during synthesis.

Capping agents cover the particle surfaces and inhibit particle agglomeration. Ahmad *et al.* [8] employed organic stabilizers as capping agents could result in tiny particles with uniform distribution. Nucleation accelerates with rising temperature, causing particles to grow larger and inclined to form clusters. Conversely, conventional approaches utilize chemical substances as capping agents to stabilize particles, which are costly and might lead to pollution.

The utilization of plant extracts in the synthesis of ZrO_2 NPs provides a highly efficient, rapid and environmental friendly approach. Alagarsamy *et al.* [9] synthesized a plant-mediated ZrO_2 NPs with pericarps from the Indian soapberry *Sapindus mukurossi*. Pala indigo plant *Wrightia tinctoria* leaves [1], pomegranate *Punica granatum* peels [4], sunflower *Helianthus annuus* seeds [10] and Indian bael *Aegle marmelos* fruits [11] have also been employed. In another study, Yuan *et al.* [12] reported the superior properties of the plant-mediated ZrO_2 NPs synthesized with a leaf extract from Gale of the wind, *Phyllanthus niruri*. The nanoparticles were small (19.25 nm) and exhibited stone-like morphologies and also demonstrated bactericidal activities against *Bacillus subtilis*, *Staphylococcus aureus*, *Escherichia coli*, *Klebsiella pneumoniae* and *Aspergillus niger*, suggesting the potential of the leaf extract in synthesizing ZrO_2 NPs with excellent characteristics.

Chloranthus erectus is a shrub that thrives in shaded areas near to streams on the forest floors of tropical and temperate zones in east Himalaya, Indo-Burma and South-East Asia. *C. erectus* leaf paste has been employed in herbal therapies to treat joint discomfort, body aches and localized swelling [13]. The plant is rich in phytochemical compounds, such as flavonoids, terpenoids, seroids, amino acids, saponins, quinones, tannins, sugar and glycosides [14]. Moreover, the total phenolic content in *C. erectus* indicated its potential as a capping agent in nanoparticles production [15]. Nonetheless, no study has been conducted to examine the effectiveness of *C. erectus* leaf during plant-mediated ZrO_2 NPs synthesis.

Typically, nanoparticles are monoclinic, tetragonal and cubic, which determine their performances in various applications. High-performance nanoparticles could be obtained by optimizing the synthesis parameters, which are crucial in regulating the growth of the particles. Several studies have extensively discussed the effects of particular conditions, including, pH, precursor and plant extract concentration, temperature and incubation time. Alahdal *et al.* [16] determined the importance of pH, precursor concentration and incubation time in copper nanoparticles manufacture. Similarly, Sukweenadhi *et al.* [17] synthesized silver nanoparticles with varying plant extract concentrations and temperatures. The natural reducing agents in the phytochemical compounds can reduce Zr ions to Zr metal, forming ZrO_2. Nevertheless, the effects of optimizing synthesis parameters on the formation of ZrO_2 NPs have not been reported, hence ideal conditions to procure high-quality ZrO_2 NPs are unavailable.

In present study, the biosynthesis of ZrO_2 NPs as efficient biological characeristics was achieved by using *C. erectus* leaf extract. This study also determined the effects of critical parameters including pH, plant extract concentration and incubation time, on the quality of ZrO_2 NPs. The optimized ZrO_2 NPs was assessed for their antibacterial and antiviral activities against pathogens.

EXPERIMENTAL

The current study employed zirconyl chloride octahydrate, sodium chloride, gentamycin (Sigma Aldrich, USA), ethanol (Chemiz, Malaysia) and deionized water without further purification. Fresh *C. erectus* leaves were gathered from Taman Negara Gunung Ledang, Johor National Park (GPS: 2.34349, 102.6225). The leaves were authenticated by a taxonomist at the Forest Research Institute Malaysia (FRIM) (PID no. 160820-12).

The pathogen cultures utilized in this study were obtained from the Unit Culture Bank, UiTM Negeri Sembilan Branch. The bacteria were cultivated in a Mueller-Hinton agar (MHA) (Sigma-Aldrich, USA). The Vero cells (ATCC, USA) were grown in 5% CO_2 environment in a Dulbecco's modified Eagle medium (DMEM) at 37 ºC. The medium was also supplemented with 10% heat-inactivated fetal bovine serum (FBS) (Gibco, New York, USA) and 1% penicillin-streptomycin (Gibco, New York, USA).

Preparation of leaf extract: The leaves samples were cleaned with distilled water and allowed to dry for a few weeks. Subsequently, the leaves were crushed into a fine powder and kept at 4 ºC in an airtight storage bottle. Subsequently, 10 g of leaf powder was mixed in a beaker with 100 mL of distilled water. The mixture was heated to 80 ºC for 2 h, left overnight and was filtrated with a no. 42 Whatman filter paper to remove any residues. The solution collected was utilized to synthesize *C. erectus* mediated ZrO_2 NPs.

Synthesis of *C. erectus* mediated ZrO_2 NPs: The green synthesis of ZrO_2 NPs using *C. erectus* leaf extract was performed according to the protocol outlined by Alagarsamy *et al.* [9]. In brief, $ZrCl_2{\cdot}8H_2O$ was mixed with 50 mL of leaf extract and stirred for 1 h. Subsequently, 2 M NaOH was added dropwise under magnetic stirring until a white precipitated formed at pH 9. After continuously stirring for another 2 h, the precipitate was centrifuged at 2000 rpm for 2 min several times and washed with ethanol and distilled water alternately after each centrifugation. The precipitate was then dried at 80 ºC overnight, with the powder calcined at 500 ºC for 3 h.

Characterization: The UV-Vis spectra of *C. erectus* mediated ZrO_2 NPs were obtained in the range of 200 and 600 nm with a T80+ UV-vis spectro-photometer (PG Instruments). A Rigaku diffractometer was utilized to obtain X-ray diffraction (XRD) data, which were employed to determine the sample unit cell parameters by employing PDXL software. The surface morphologies and shapes of the green synthesized ZrO_2 NPs were examined with an energy dispersive X-ray (EDX)-equipped scanning electron microscope (SEM) (Hitachi TM3030 PLUS model) and transmission electron microscope (TEM) (Talos L120C). A Fourier-Transform infrared (FTIR) (Perkin-Elmer)

analysis within the 4000–400 cm^{-1} range was also conducted to determine the significant functional groups in the *C. erectus* mediated ZrO_2 NPs.

Antibacterial activities

Bacterial strains: Antibacterial activities of *C. erectus* mediated ZrO_2 NPs synthesized in this study were established against pathogenic isolates of Gram-positive (*S. aureus* and *B. cereus*) and Gram-negative bacteria (*P. aeruginosa*, *E. coli* and *K. pneumoniae*). The strains were obtained from the Bank Culture Unit, Universiti Teknologi MARA Cawangan Negeri Sembilan, Malaysia.

Antibacterial properties: The antibacterial activities of the *C. erectus* mediated ZrO_2 NPs and standard antibiotic (gentamycin, 10 µg/mL) were evaluated *via* the disc diffusion method [4] with slight modifications. First, a 250 mL bacterial suspension adjusted to 10^6 CFU/mL was combined with 30 mL molten HMA. After the mixture solidified, a sterilized disc (6 mm) containing ZrO_2 NPs (0.5 mg/mL) of different concentrations, ranging from 50 to 250 µg/mL, was transferred aseptically to the surface of inoculated agar. A standard antibiotic (gentamycin) and DMSO (negative control) were also applied. The inhibition zone diameters were then determined in mm. Subsequently, the plates were incubated at 37 ºC for 24 h and each sample was assessed in triplicates.

Antiviral activities

Viral preparation: In this study, the DENV-2 stock was prepared based on the guidelines reported by Kothai *et al.* [18] with minor alterations. The Vero cells were seeded at 3×10^6 per well in a 6-well plate with 2 mL medium. The plate was left for 24 h in a 5% CO_2 incubator until a confluent monolayer of cells was observed through a microscope. The virus growth medium utilized in the current study was prepared in a 15 mL tube by combining serum-free DMEM with 0.2% FBS and 1% pen-strep. The Vero cell monolayer in the 6-well plate was deterged with phosphate-buffered saline twice.

The cells were infected with the DENV-2 inoculum at 0.1 multiplicity of infection (MOI) for 1 h at 37 ºC and shaken front-to-back and side-to-side every 15 min. After 1 h of incubation, 1.5 mL of virus growth medium was added to each well and the 6-well plate was incubated in a 37 ºC 5% CO_2 incubator for 72 h. The infected cultures were checked daily to observe any cytopathic effects (CPE). Once 80% of the cells were detached from the surfaces, the virus-containing supernatants were harvested and centrifuged at 500*x* g for 5 min and the virus was then stored in a –80 ºC freezer.

Preparation of different *C. erectus* mediated ZrO_2 NPs concentrations: In this study, 20 mg of biosynthesized nanoparticles were added to 1000 µL autoclaved distilled water to prepare a 20000 µg/mL ZrO_2 NPs solution. A two-fold serial dilution was performed to prepare nanoparticles of different concentrations (500, 250, 125 62.50, 31.25, 15.63, 7.81 and 0 µg/mL).

Cell cytotoxicity assay: The cytotoxic effects of the nanoparticles synthesized were evaluated through a 3-(4,5-dimethylthiazol-2-yl)-5-(3-carboxymethoxyphenyl)-2-(4-sulfophenyl)-2*H*-tetrazolium (MTS) assay (Promega, USA). The procedure was performed according to the manufacturer's instructions. Vero cells at 1×10^5 per well were seeded in a 96-well plate with 100 µL of the growth media. The 96-well plate was left for 24 h until a confluent monolayer of cells was observed under a microscope. The used medium in the plate was then removed. The wells were washed with phosphate buffer solution (PBS) to remove the remaining medium. Subsequently, 100 µL of the synthesized ZrO_2 NPs were added to the 96-well plates. Each ZrO_2 NPs concentration was evaluated in triplicates and the control group in this study only received cell culture media.

After being incubated for 72 h, each well was added with 20 µL MTS reagent (Promega, USA) and incubated again in a 5% CO_2 incubator (Labserv, Thermo-Fisher Scientific, USA) for 1 h. A microplate reader (BioTek Synergy, USA) was utilized to determine the amount of solubilized formazan crystals formed in each well. The viability (VR) of the nanoparticles-treated cells was calculated according to the formula $VR = A/A_0$, where A denotes the absorbance of the experimental group and A_0 represents the absorbance of the control group. The average absorbance of the control cells (treated with only the cell culture medium) was considered at 100% viability. Wells with 80% or more viability following the treatments were considered non-cytotoxic.

Cytopathic effect reduction assay: Vero cells of 1×10^5 per well were seeded in a 96-well plate with 100 µL DMEM media. The 96-well plate was left for 24 h until a confluent monolayer of cells was observed under a microscope. In an Eppendorf tube, 400 µL of 2% DMEM was mixed with 400 µL of ZrO_2 NPs solution. The used media in the plate was discarded and washed with PBS before 50 µL of prepared synthesized ZrO_2 NPs solution at different concentrations and 50 µL of DENV-2 solution with MOI = 0.1 were pipetted into the wells and resuspended to thoroughly mix them. Each ZrO_2 NPs solution concentration and the virus and cell controls were evaluated in triplicates. Subsequently, the treated cells were incubated and observed daily for the presence of cytopathic effect. A microplate reader was employed to read the absorbance of the 96-well plate at 490 nm. The cytopathic inhibition percentage of each sample was calculated according to eqn. 1:

$$\text{Cytopathic inhibition (\%)} = \frac{\text{OD of [T} - \text{VC]}}{\text{OD of [CC} - \text{VC]}} \quad (1)$$

where OD represents optical density, T is the cells treated with the compound, CC denotes cell control and VC is the virus control [19].

Statistical analysis: The experimental data obtained from the cell cytotoxic and cytopathic effect reduction assays conducted in this study were statistically evaluated with GraphPad Prism version 9 (GraphPad Software Inc., San Diego, USA). The information acquired from the cell cytotoxic assessment was then analyzed with a four-parameter dose-response curve fit to derive the half-maximal cytotoxic concentration (CC_{50}) and half-maximal inhibitory concentration (IC_{50}) of each sample. The maximum non-toxic dose (MNTD) value, where 95% of cells were viable was also obtained from the cell cytotoxicity dose-response curve. Consequently, the CC_{50}-to-IC_{50} ratio of

the compound was determined to establish the selectivity index (SI) value.

RESULTS AND DISCUSSION

Effect of pH: The effects of different parameters employed were determined with the UV-Vis spectroscopy between 200 and 600 nm (Fig. 1). The formation of biosynthesized ZrO_2 NPs was confirmed when an absorbance band at 214 nm was observed.

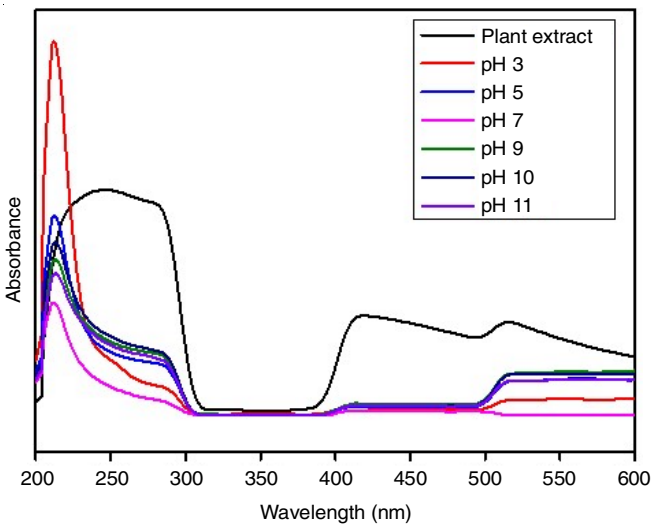

Fig. 1. UV-Vis spectroscopy at different pH during synthesis *C. erectus*-ZrO_2 NPs

Plant extract concentration: The optimal sample concentration in this study that generated the maximum UV-Vis absorbance response was 5 g/150 mL of ZrO_2 NPs (Fig. 2). Plant extract concentration has demonstrated significant influences on the shape and size of nanoparticles.

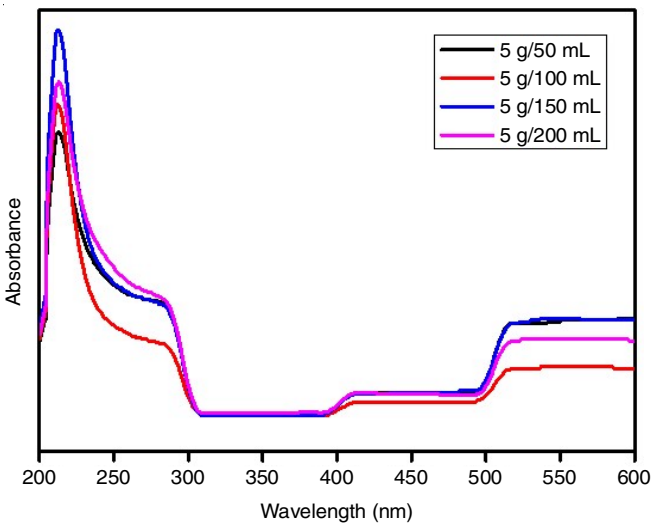

Fig. 2. UV-vis spectroscopy at different concentrations of plant extract during synthesis *C. erectus*-ZrO_2 NPs

Incubation time: In this study, the effects of different incubation times (3, 6 and 24 h) were evaluated utilizing the optimized pH and plant extract concentration. Fig. 3 illustrates that the

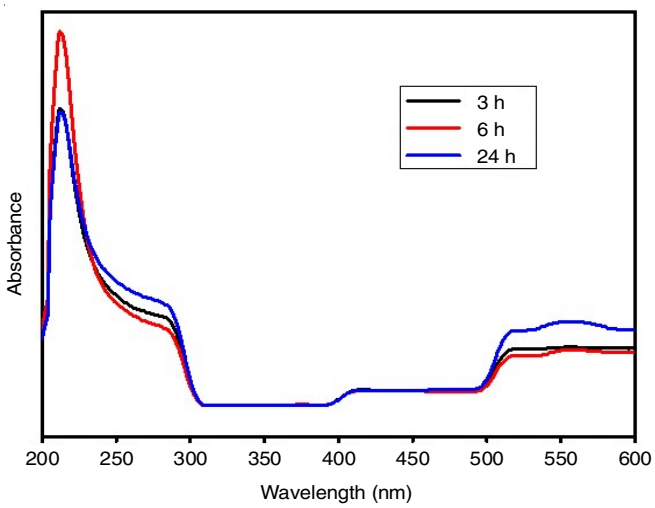

Fig. 3. UV-Vis spectroscopy at incubation times during synthesis of *C. erectus*-ZrO_2 NPs

ideal absorbance signal was obtained after 6 h of incubation, which allowed the precursor to react with NaOH and the plant extract. Alagarsamy *et al.* [9] also demonstrated the importance of the incubation period in producing excellent ZrO_2 NPs.

XRD studies: The XRD spectra in Fig. 4 demonstrate the biogenic capped and uncapped ZrO_2 NPs. The data revealed distinct diffraction peaks at 30.29º, 35.32º, 50.44º, 60.28º, 63.12º and 82.28º, corresponding to the (011), (110), (020), (121), (202) and (220) diffraction planes. These findings are matched with the standard diffraction data provided in JCPDS card No.: 00-050-1089. On average, the crystallite size of the synthesized *C. erectus* mediated ZrO_2 NPs in the current study was 9.96 nm. Nevertheless, the uncapped ZrO_2 NPs documented an average crystallite size of 12.28 nm, slightly bigger than its capped counterpart. Moreover, the biosynthesized ZrO_2 NPs in the current study was also smaller (34.33 nm) than the ZrO_2 NPs synthesized from native *Enterobacter* sp. [3].

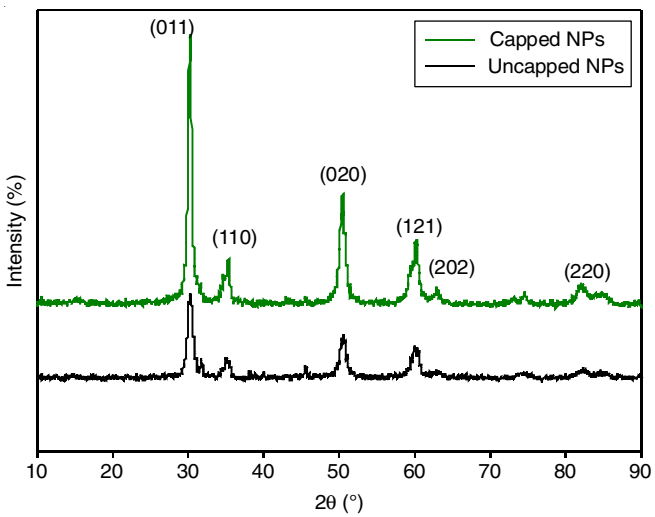

Fig. 4. XRD spectra of uncapped and capped *C. erectus*-ZrO_2 NPs

Based on the XRD data, the nanoparticles prepared in this study had tetragonal crystal systems, which was in accordance with the report of Saraswathi & Santhakumar [20]. The XRD

diffraction peaks were also significantly similar to the ZrO_2 NPs prepared utilizing Indian bael fruit extract [11]. Nonetheless, the uncapped ZrO_2 NPs peaks were more intense than the *C. erectus* capped nanoparticles. The uncapped nanoparticles also had no peak corresponding to (220), indicating the effectiveness of *C. erectus* to produce substantial ZrO_2 NPs crystallinity. The synthesized ZrO_2 NPs diffraction pattern exhibited higher intensity peaks than the uncapped nanoparticles. The results were similar to the report by Putri *et al.* [21], who also synthesized green CeO_2 NPs.

TEM studies: The morphology of the *C. erectus* mediated ZrO_2 NPs and uncapped ZrO_2 NPs procured in this study was established with TEM (Fig. 5). Agglomerated spherical-shaped particles were observed. The particle size distribution analysis recorded 6.06 ± 2.18 nm. The assessment was performed utilizing Image-J software on 100 random particles and the mean particle size range was determined with a histogram. The images closely matched the size calculated from XRD by employing Scherrer's equation. According to Alagarsamy *et al.* [9], the size of nanoparticles contributes to its stabilisation phase. ZrO_2 NPs are more stable when in monoclinic crystal structures if their size range is over 20 nm. On the other hand, particles between 7 and 20 nm exhibit tetragonal crystal structures. The average size of the nanoparticles in this study was 6.73 ± 1.44 nm, which parallels the tetragonal phase.

FTIR studies: The infrared spectra of *C. erectus* leaf extract and biosynthesized ZrO_2 NPs were recorded to identify the functional groups of the biomolecules responsible for the synthesis and stabilization of the nanoparticles. The ZrO_2 NPs documented distinct the functional groups at 3396 and 1611 cm^{-1} (Fig. 6). The observation indicated that the plant extract contained significant functional groups derived from its phytochemical compounds, which had a pivotal role in stabilizing the *C. erectus* mediated ZrO_2 NPs.

The band observed at 486 cm^{-1} was assigned to the formation of ZrO_2 NPs. The *C. erectus* leaf extract also exhibited

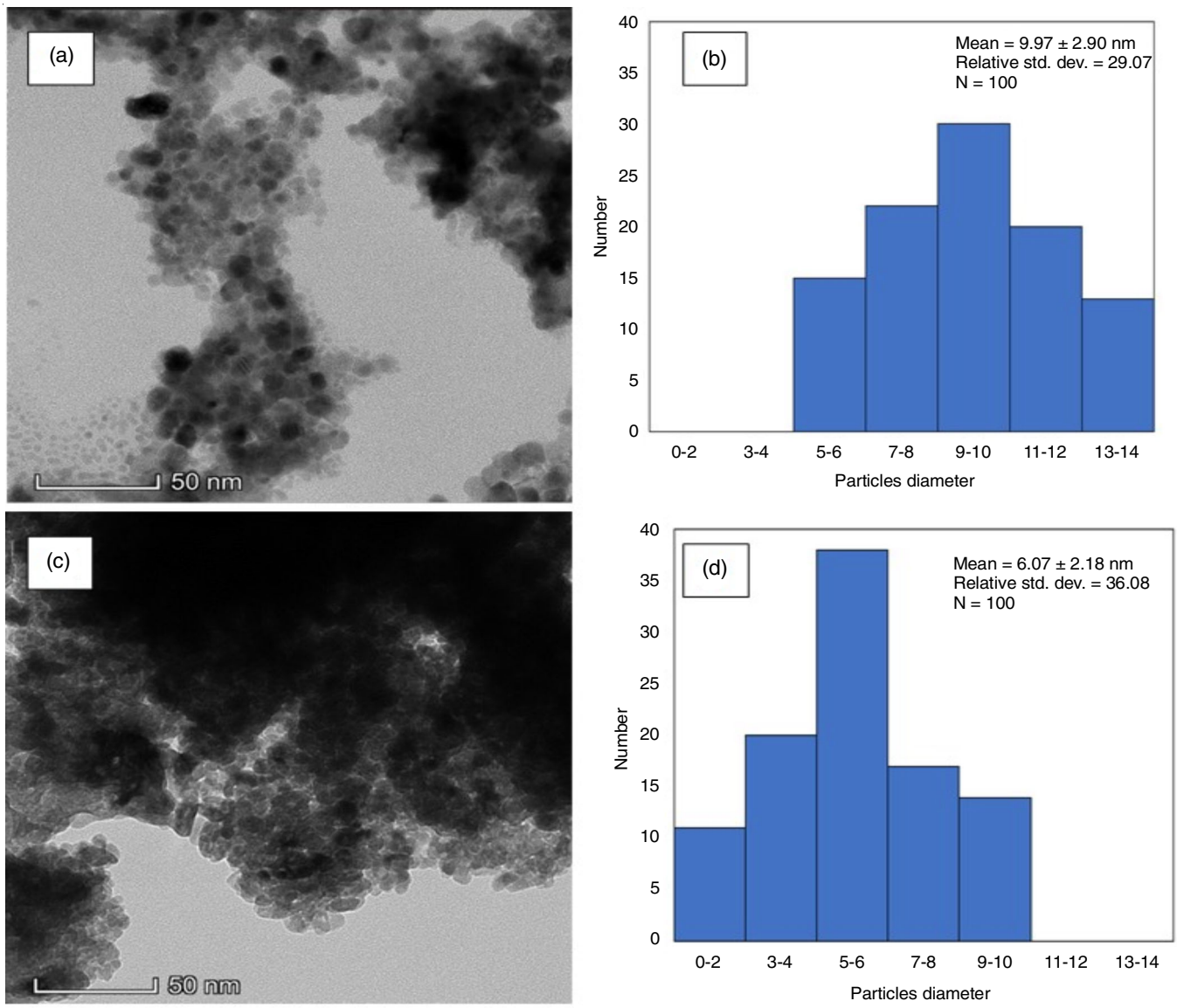

Fig. 5. (a) TEM image of uncapped ZrO_2 NPs, (b) histogram plot of uncapped ZrO_2 NPs, (c) TEM image of capped *C. erectus*-ZrO_2 NPs and (d) histogram plot of capped *C. erectus*-ZrO_2 NPs

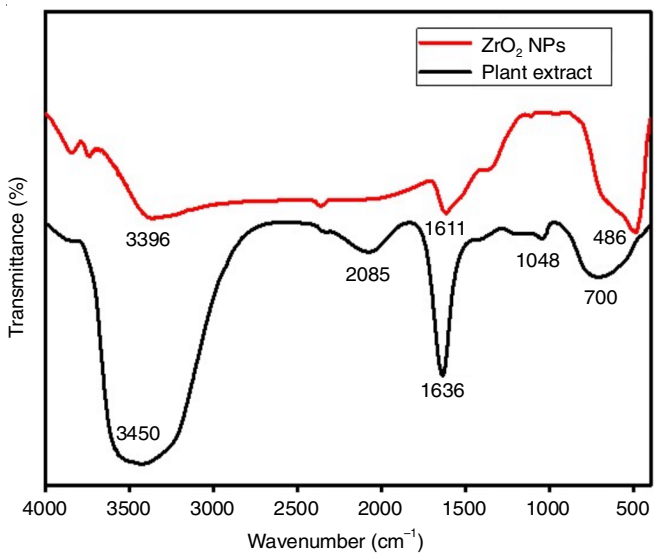

Fig. 6. FTIR spectra of *C. erectus*-ZrO_2 NPs

significant peak at 1636 cm^{-1} due to the C=O carboxyl group stretching. The broad O-H band at 3450 cm^{-1} indicated by the bonds linked to the secondary metabolites suggested flavonoids, polyphenols and alkaloids in the plant extract, which might stabilized the ZrO_2 NPs formed. According to Karthik *et al.* [22], the phytochemical compounds in plant extracts are critical as a capping agent as they could protect the nanoparticles by suppressing the cluster developments. These findings were in accordance with the data recorded by Goyal *et al.* [10], which synthesized ZrO_2 NPs with *H. annus* using seed extract.

Antibacterial activities: The present study employed the agar well diffusion method to assess the antibacterial activities of plant medidated synthesized ZrO_2 NPs against *E. coli*, *K. pneumoniae*, *S. aureus* and *B. subtilis*. Gentamycin, the preferred bacterial infection treatment was also utilized as a control (broad spectrum). The results indicated that the most significant inhibition zone was observed in the absence of the nanoparticles. Nevertheless, the synthesized ZrO_2 NPs demonstrated *K. pneumoniae* growth-reducing potential. The nanoparticles did not affect *E. coli*, *S. aureus* and *B. subtilis*. Increasing the concentration of nanoparticles resulted in enhanced inhibition zones against *K. pneumoniae*, measuring 1.23 mm at 200 µg/mL (Table-1). The positively charged Zr ions effectively caused cell death by disrupting the negatively charged bacterial cell wall [23]. The electromagnetic attractions between microorganisms with negative charges and positively charged metal oxides lead to oxidation and the death of microorganisms [24].

The sulphated ZrO_2 NPs synthesized by Mftah *et al.* [25] demonstrated the considerable antibacterial actions against methicillin-resistant *S. aureus* and *P. aeruginosa* (30 nm ZOI), *B. subtilis* and *S. choleraesuis*. In another study, Banerjee *et al.* [26] found that ZrO_2 NPs exhibited antibacterial activities against *E. coli* bacteria but not *S. aureus* or fungi. The findings documented in this study indicated that the *C. erectus* medidated ZrO_2 NPs could be employed as an anti-bacterial agent against the Gram-negative *K. pneumoniae* bacteria also. The NPs improved the generation of reactive oxygen species (ROS), eradicating bacterial cells. Nevertheless, the capacity of the nanoparticles to bind to bacteria is contingent upon size and dosage. Smaller particles with larger surface volumes facilitated extensive contact areas with the microbes. The inherent ZrO_2 characteristics significantly enhance the biological and chemical properties of its nanoparticles, rendering them considerably effective and robust bacteriostatic materials.

Antiviral properties: The cytotoxicity of the green synthesized *C. erectus* medidated ZrO_2 NPs was also determined with Vero cells in an MTT assay. The cells were treated with varying concentrations of the nanoparticles, which ranged between 0 and 500 µg/mL.The evaluation revealed significant ZrO_2 NPs cytotoxicity at concentrations > 314.30 µg/mL after 72 h of incubation (Fig. 7a). The substantial CC_{50} value suggested that the synthesized ZrO_2 NPs possessed relatively low toxicity towards the Vero cells. Although the cytotoxicity of metal nanoparticles is dependent on different factors, such as shape, size, nanoparticles concentration, exposure time and cell types [27], some cells, including macrophages, fibroblasts and epithelial cells, are more sensitive towards metal nanoparticles [28].

The maximum non-toxic dosage (MNTD) value refers to the maximum dosage of a medicine utilized to produce serious or unacceptably negative side effects [29]. The *C. erectus* mediated ZrO_2 NPs produced in this study recorded a higher MNTD value (290.56 µg/mL) than medicinal plant-synthesized Ag NPs, which recorded 30-250 µg/mL [30]. A cytopathic effect reduction assay was also performed to determine the *C. erectus* mediated ZrO_2 NPs abilities to inhibit DENV-2 infections. Smee *et al.* [31] reported the capabilities of the assessment to assess the antiviral activities of compounds of interest against DENV-2. In this study, the *C. erectus* mediated ZrO_2 NPs documented 229.00 µg/mL IC_{50}, indicating a weak antiviral activity against DENV-2 (Fig. 7b). Varying concentrations of the synthesized ZrO_2 NPs also did not substantially inhibit the cytopathic effect (CPE) caused by DENV-2 viral infections. Moreover, increasing the ZrO_2 NPs concentration to 500 µg/

TABLE-1
ANTIBACTERIAL ACTIVITIES OF THE *C. erectus*-ZrO_2 NPs AGAINST BACTERIA PATHOGENS

Bacterial pathogen	ZrO_2 NPs concentration (µg/mL)					Gentamycin (µg/mL)
	50	100	150	200	250	10
E. coli	NIZ	NIZ	NIZ	NIZ	NIZ	4.00 ± 0.05
K. pneumonia	NIZ	NIZ	NIZ	1.2 ± 0.23*	NIZ	2.73 ± 0.14
S. aureus	NIZ	NIZ	NIZ	NIZ	NIZ	2.51 ± 0.10
B. subtilis	NIZ	NIZ	NIZ	NIZ	NIZ	3.33 ± 0.05

Note: NIZ: No inhibition zone, NS: not significant, all data represent mean ± standard deviation (*$p < 0.05$) of three replicates and all comparisons were conducted with gentamicin as the standard drug.

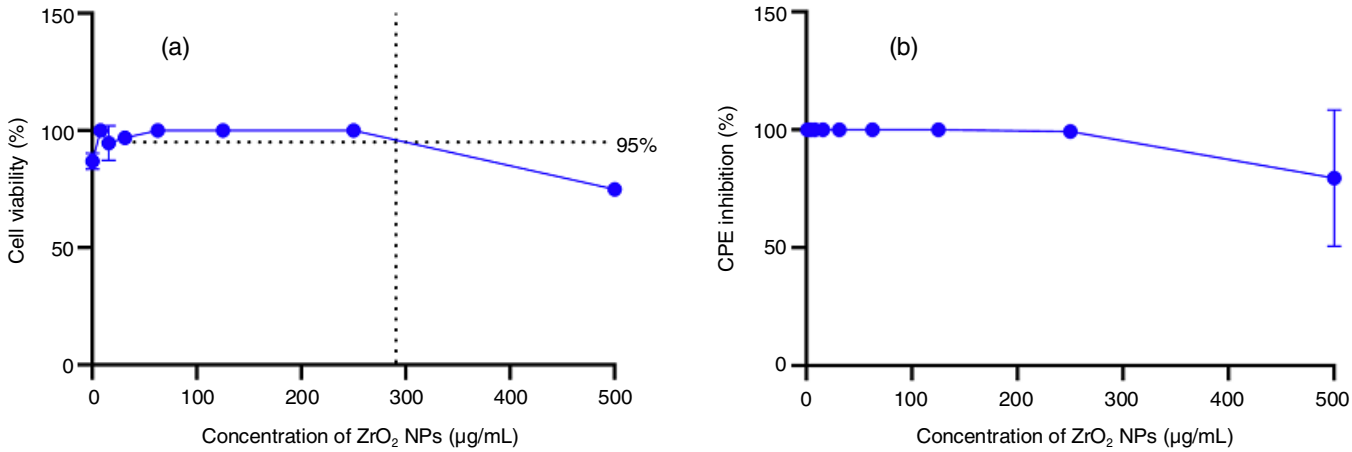

Fig. 7. *C. erectus*-ZrO_2 NPs exhibit low antiviral activity against DENV-2. (a) Cytotoxicity assay of *C. erectus*-synthesized ZrO_2 NPs at various concentrations on vero cells at 96 h post-treatment using MTS assay. Results from triplicates are shown as the percentage of cell viability against different concentrations of *C. erectus*-ZrO_2 NPs. (b) Cytopathic effect (CPE) reduction assay against DENV-2 by MTS assay. Vero cells were treated with increasing concentrations of *C. erectus*-ZrO_2 NPs for 4 days. The data are normalised to non-treated control cells which were set to be 100% in triplicate assay. Error bars represent the standard deviation of the mean

mL only yielded a slight CPE inhibitory effect reduction. The phenomenon might results from cell toxicity (Fig. 7a-b).

Generally, the SI values are employed as a pre-clinical screening technique for drugs and a pertinent indicator in preliminary procedures for further assessments. The data is obtained by calculating CC_{50}-to-IC_{50} ratios. A significant SI is an early pharmacological success predictor of the relative safety of a drug product for clinical applications [32]. Ideally, a compound with a considerable SI value would kill the virus before the host cells, indicating the selectivity of the towards the virus instead of the host cells.

Although the IC_{50} of *C. erectus* mediated ZrO_2 NPs synthesized in the current study was higher (229.00 µg/mL) than the Ag NPs on SARS-CoV2 (0.005 µg/mL), its SI value was significantly lower at 1.37 than the 12.40 reported by Flórez-Álvarez *et al.* [33]. The low SI value indicated that *C. erectus* mediated ZrO_2 NPs had a low potential antiviral activity against DENV-2 virus. The nanoparticles were also observed aggregated when viewed under a microscope (data not shown) with inconsistent sizes, which might have decreased their antiviral effectiveness.

Conclusion

The current study successfully synthesized and characterized *C. erectus* mediated ZrO_2 NPs utilizing *C. erectus* leaf aqueous extract. The biosynthesized demonstrated a significantly discernible UV-vis absorption peak at 214 nm. The present study also determined the optimized conditions for producing high-performance ZrO_2 NPs, which were pH 5, 5 g/150 mL of the plant extract and 6 h of incubation. The UV-vis absorption band confirmed the ideal conditions. Furthermore, the purity, morphology and average particle size of *C. erectus* mediated ZrO_2 NPs were characterized by XRD, FTIR, TEM, SEM and EDAX. Nevertheless at 200 µg/mL, *C. erectus* mediated ZrO_2 NPs exhibited low antibacterial efficacy against *K. pneumoniae* and antiviral activities against DENV-2 viruses. Quantitative approaches, such as plaque reduction assay, could be conducted to obtain more information, including the degree of inhibition of viral replication of serially diluted *C. erectus* mediated ZrO_2 NPs. An immunofluorescent assay could also be performed to investigate how the NPs affect DENV-2 virus antigen expressions on Vero cell surfaces.

ACKNOWLEDGEMENTS

This study was funded by Universiti Teknologi MARA under the Lestari SDG Triangle 2021 Research Grant [grant no. 600-RMC/LESTARI SDG-T 5/3 (014/2021)]. The authors express their gratitude to the Faculty of Applied Science UiTM Shah Alam and the Centre for Research and Instrumentation Management (CRIM) for providing the analytical facilities. The authors also thank the Johor National Park for allowing plant sample collection and UiTM Negeri Sembilan Branch for granting permission to utilize its facilities throughout the study.

CONFLICT OF INTEREST

The authors declare that there is no conflict of interests regarding the publication of this article.

REFERENCES

1. N. Al-Zaqri, A. Muthuvel, M. Jothibas, A. Alsalme, F.A. Alharthi and V. Mohana, *Inorg. Chem. Commun.*, **127**, 108507 (2021); https://doi.org/10.1016/j.inoche.2021.108507
2. N.S. Tapak, M.A. Nawawi, E.T.T. Tjih, Y. Mohd, A.H.A. Rashid, N.A. Yusof, J. Abdullah and N.M. Ahmad, *Mater. Today Commun.*, **33**, 104142 (2022); https://doi.org/10.1016/j.mtcomm.2022.104142
3. T. Ahmed, H. Ren, M. Noman, M. Shahid, M. Liu, M.A. Ali, J. Zhang, Y. Tian, X. Qi and B. Li, *NanoImpact*, **21**, 100281 (2021); https://doi.org/10.1016/j.impact.2020.100281
4. T.P. Chau, G.R. Veeraragavan, M. Narayanan, A. Chinnathambi, S.A. Alharbi, B. Subramani, K. Brindhadevi, T. Pimpimon and S. Pikulkaew, *Environ. Res.*, **209**, 112771 (2022); https://doi.org/10.1016/j.envres.2022.112771
5. L.S. Reddy Yadav, T. Ramakrishnappa, J.R. Pereira, R. Venkatesh and G. Nagaraju, *Mater. Today Proc.*, **49**, 686 (2022); https://doi.org/10.1016/j.matpr.2021.05.172

6. S. Tantuvoy, M. Kumar and I. Nambi, *J. Environ. Chem. Eng.*, **11**, 110721 (2023); https://doi.org/10.1016/j.jece.2023.110721
7. F. Ordóñez, F. Chejne, E. Pabón and K. Cacua, *Ceram. Int.*, **46**, 11970 (2020); https://doi.org/10.1016/j.ceramint.2020.01.236
8. H.A. Ahmad, N.M. Saiden, E. Saion, R.S. Azis, M.S. Mamat and M. Hashim, *J. Magn. Magn. Mater.*, **428**, 219 (2017); https://doi.org/10.1016/j.jmmm.2016.12.047
9. A. Alagarsamy, S. Chandrasekaran and A. Manikandan, *J. Mol. Struct.*, **1247**, 131275 (2022); https://doi.org/10.1016/j.molstruc.2021.131275
10. P. Goyal, A. Bhardwaj, B.K. Mehta and D. Mehta, *J. Indian Chem. Soc.*, **98**, 100089 (2021); https://doi.org/10.1016/j.jics.2021.100089
11. V. Lakshmi Ranganatha, G. Nagaraju, J.S. Vidya, H.N. Deepakumari, D.M. Gurudutt and C. Mallikarjunaswamy, *Mater. Today Proc.*, **62**, 5067 (2022); https://doi.org/10.1016/j.matpr.2022.02.407
12. Y. Yuan, Y. Wu, N. Suganthy, S. Shanmugam, K. Brindhadevi, A. Sabour, M. Alshiekheid, N.T. Lan Chi, A. Pugazhendhi and R. Shanmuganathan, *Food Chem. Toxicol.*, **168**, 113340 (2022); https://doi.org/10.1016/j.fct.2022.113340
13. H. Tag, N.D. Namsa, A.K. Das, P. Kalita and S.C. Mandal, *J. Ethnopharmacol.*, **126**, 371 (2009); https://doi.org/10.1016/j.jep.2009.08.015
14. N.A. Hasan, S. Ariffin, A.M. Azzeme, N.I. Hasbullah, M.Z. Nawahwi and I.H. Bin Zemry, *Mater. Today Proc.*, **88**, 6 (2023); https://doi.org/10.1016/j.matpr.2023.01.365
15. I.H. Zemry, N.A. Hasan, N.I. Hasbullah, M.Z. Nawahwi, A. Mohamad Azzeme, S.N.D. Ahmad and S. Ariffin, *J. Exp. Biol. Agric. Sci.*, **11**, 75 (2023); https://doi.org/10.18006/2023.11(1).75.80
16. F.A.M. Alahdal, M.T.A. Qashqoosh, Y.K. Manea, R.K.A. Mohammed and S. Naqvi, *Sustain. Mater. Technol.*, **35**, e00540 (2023); https://doi.org/10.1016/j.susmat.2022.e00540
17. J. Sukweenadhi, K.I. Setiawan, C. Avanti, K. Kartini, E.J. Rupa and D.C. Yang, *S. Afr. J. Chem. Eng.*, **38**, 1 (2021); https://doi.org/10.1016/j.sajce.2021.06.008
18. R. Kothai, B. Arul and V. Anbazhagan, *Appl. Biochem. Biotechnol.*, **195**, 3747 (2023); https://doi.org/10.1007/s12010-022-03966-w
19. Y. Kim, E.Y. Oh, S. Park and S.M. Lee, *J. Bacteriol. Virol.*, **51**, 200 (2021); https://doi.org/10.4167/jbv.2021.51.4.200
20. V. Sai Saraswathi and K. Santhakumar, *J. Photochem. Photobiol. B*, **169**, 47 (2017); https://doi.org/10.1016/j.jphotobiol.2017.02.023
21. G. Eka Putri, Y. Rilda, S. Syukri, A. Labanni and S. Arief, *J. Mater. Res. Technol.*, **15**, 2355 (2021); https://doi.org/10.1016/j.jmrt.2021.09.075
22. M. Karthik, C. Ragunath, P. Krishnasamy, D. Queen Paulraj and V. Ramasubramanian, *Inorg. Chem. Commun.*, **157**, 111422 (2023); https://doi.org/10.1016/j.inoche.2023.111422
23. N. Tabassum, D. Kumar, D. Verma, R.A. Bohara and M.P. Singh, *Mater. Today Commun.*, **26**, 102156 (2021); https://doi.org/10.1016/j.mtcomm.2021.102156
24. H. Zhang and G. Chen, *Environ. Sci. Technol.*, **43**, 2905 (2009); https://doi.org/10.1021/es803450f
25. A. Mftah, F. H alhassan, M. sadiq Al-Qubaisi, M. Ezzat El Zowalaty, T.J. Webster, M. Sh-eldin, A. Rasedee, Y.H. Taufiq-Yap and S.S. Rashid, *Int. J. Nanomedicine*, **10**, 765 (2015); https://doi.org/10.2147/IJN.S66058
26. K. Banerjee, M. Prithviraj, N. Augustine, S.P. Pradeep and P. Thiagarajan, *J. Chem. Pharm. Sci.*, **9**, 1186 (2016).
27. A. Sani, C. Cao and D. Cui, *Biochem. Biophys. Rep.*, **26**, 100991 (2021); https://doi.org/10.1016/j.bbrep.2021.100991
28. Y. Pan, S. Neuss, A. Leifert, M. Fischler, F. Wen, U. Simon, G. Schmid, W. Brandau and W. Jahnen-Dechent, *Small*, **3**, 1941 (2007); https://doi.org/10.1002/smll.200700378
29. N.A. Rahman, Hadinur, S. Muliawan, N.N. Rashid, M. Muhamad and R. Yusof, *Dengue Bull.*, **30**, 260 (2006).
30. V. Sharma, S. Kaushik, P. Pandit, D. Dhull, J.P. Yadav and S. Kaushik, *Appl. Microbiol. Biotechnol.*, **103**, 881 (2019); https://doi.org/10.1007/s00253-018-9488-1
31. D.F. Smee, B.L. Hurst, W.J. Evans, N. Clyde, S. Wright, C. Peterson, K.-H. Jung and C.W. Day, *J. Virol. Methods*, **246**, 51 (2017); https://doi.org/10.1016/j.jviromet.2017.03.012
32. M. Ali, M.E. van Gent, A.M. de Waal, B.R. van Doodewaerd, E. Bos, R.I. Koning, R.A. Cordfunke, J.W. Drijfhout and P.H. Nibbering, *Int. J. Mol. Sci.*, **24**, 2867 (2023); https://doi.org/10.3390/ijms24032867
33. L. Flórez-Álvarez, J.C. Hernandez, W. Zapata-Builes, J.I. Charry-Zuluaga, J.R. Jaramillo, N.A. Taborda, J.D. Gonzalez, L.L. Martínez and L.M. Yasssin-Noreña, *Iatreia.*, **36**, 5 (2022); https://doi.org/10.17533/udea.iatreia.188